Sustainable Preparation of AuAg alloy@AgBr Janus Nanoparticles via Dissipative Self-assembly for Photocatalysis

Kanica Sharma,[a] Harjinder Singh,[a] Gurbir Singh,[a] Navdeep Kaur,[b] Pratap Kumar Pati,[b] Kuldeep Singh,[c] Arvind Kumar,[c] and Tejwant Singh Kang*,[a]

[a]*Department of Chemistry, UGC-Centre for Advance Studies – II, Guru Nanak Dev University, Amritsar, 143005, India.*

[b]*Department of Biotechnology, Guru Nanak Dev University, Amritsar, Punjab 143005, India.*

[c]*Academy of Scientific and Industrial Research (ACSIR), Ghaziabad, 201002, CSIR-Central Salt and Marine Chemicals Research Institute (CSIR), G. B. Marg, Bhavnagar, Gujarat 364002, India*

Supplementary information

**To whom correspondence should be addressed: e-mail*: tejwantsinghkang@gmail.com; tejwant.chem@gndu.ac.in Tel: +91-183-2258802-Ext-3291

1. Annexure S1

1.1 Materials: Silver nitrate (>99%), gold(III) chloride trihydrate (>99.9% trace metal basis), and *p*-benzoquinone (>98%, reagent grade) were purchased from Sigma-Aldrich Pvt. Ltd., India. Cetyltrimethylammonium bromide (99%), isopropyl alcohol (99.8%), and ethylenediaminetetraacetic acid (disodium salt) (99%) were procured from Loba Chemie Pvt. Ltd., India. Ascorbic acid (99.7%) and sodium hydroxide pellets were bought from Sisco Research Laboratories Pvt. Ltd., India. Rhodamine B dye was obtained from s d Fine-Chem Ltd., India. All materials were used as received.

1.2 Preparation of AuAg alloy@AgBr JNPs: The AuAg alloy@AgBr JNPs were synthesized in a one-pot three-step process. At first, aqueous colloidal sol of AgBr was prepared by adding CTAB (10 mM) to 0.5 mM solution of $AgNO_3$ with constant stirring at 700 rpm for 1 hour. 0.2 mM $HAuCl_4$ was then added to the colloidal sol of AgBr capped by CTAB and kept for stirring at 700 rpm for 1 hour. In the final step, aqueous ascorbic acid (8 mM) was added to the reaction mixture and subjected to the same stirring conditions for 30 minutes in the dark. After the addition of ascorbic acid, the reaction mixture was covered with aluminum foil and reserved in dark conditions before its exposure to sunlight for photoreduction. Visual color change in the reaction mixture was seen after 30 minutes of sunlight irradiation, indicating the formation of AuAg alloy@AgBr JNPs. These formed colloidal particle suspensions were centrifuged at 10000 rpm for 20 minutes to precipitate out the desired AuAg alloy@AgBr [JNP-1] formed. To remove all the unreacted precursors, the JNPs were washed with distilled water and then ethanol three times each. To investigate and compare the effects of pH on the growth and properties of the particles, the procedure was repeated by using an aqueous solution of Au(III) at pH ~ 10. For this, 0.2 mM aqueous solution of $HAuCl_4$ was prepared, and aqueous NaOH was added to achieve pH ~ 10. The disappearance of the characteristic yellow color of $HAuCl_4$ marks the formation of $Au(OH)_4^-$, which was then used for the preparation of AuAg alloy@AgBr JNPs in the basic medium [JNP-2].

1.3 Characterization of AuAg alloy@AgBr JNPs: The formation of AuAg alloy@AgBr JNPs was monitored with the help of UV-Vis absorption spectra recorded via UV-Vis-NIR Spectrophotometer (CARY 5000 UV-Vis-NIR) in a quartz cuvette having a path length of 1 cm in the wavelength range of 200-800 nm. To study the growth mechanism of the particles, time-

dependent UV absorption spectra were recorded by taking aliquots of 700µl each from reaction mixtures before and during sunlight exposure at different time intervals. The ^{1}H Nuclear Magnetic Resonance (NMR) spectroscopy experiment was performed using a Brüker Ascend 500 spectrometer (AVANCE III HD console) for the metal-CTAB complex formed at every stage of the reaction to understand the interactions of metal ions with CTAB responsible for the growth mechanism of the JNPs. The chemical shift values, reported in δ units (ppm), were measured by taking $CDCl_3$ as an external standard and setting δ value at 0.00 ppm corresponding to the singlet observed for Trimethyl silane (TMS) as the reference. Rigaku Xpert Pro X-Ray Diffractometer with Cu source (λ = 1.54 A°) was utilized to investigate the X-ray diffraction pattern of the prepared JNPs in the 2θ range of 5°-90° at a scanning rate of 2° min^{-1}. Malvern Light Scattering instrument (Zetasizer Nano Series Nano-ZS) was employed to determine the size of the JNPs by taking an aqueous dispersion of the sample in a quartz cuvette of unit path length via backscattering at 173°. The same instrument was used for measuring Zeta (ζ)-potential using a dip cell for zeta potential. Transmission electron microscopy (TEM) was performed employing JEOL JEM 2100 PLUS equipment at 200kV. The JNPs were dispersed in ethanol, and a single drop of the dispersion was cast on a carbon-coated grid (300 mesh) and dried for 24 hours before performing TEM measurement. The same ethanolic dispersion of the particles was drop cast on a clean glass surface and dried for 24 hours at room temperature followed by silver coating for Scanning Electron Microscopy (SEM) measurements done by employing Zeiss Ultra 55-Limited Edition SEM. X-ray Photoelectron Spectroscopy (XPS) was executed with a Thermo-Scientific NEXSA Spectrometer using a monochromatic Al Kα X-ray source operated at 1486.6 eV with magnetic focusing and charge neutralizer. Thermo-Avantage v5.9925 software and Thermo-Avantage v5.9921 software were used to analyze the spectra obtained and curve-fitting.

1.4 Photocatalytic Activity of AuAg alloy@AgBr JNPs: Rhodamine B (RhB) was used as a model water pollutant to test the photocatalytic efficiency of the JNPs in the presence of sunlight. 15 mg of the material was dispersed in 30 ml of 0.01 mM aqueous solution of RhB and kept for stirring for about 1 hour in dark conditions to reach adsorption-desorption equilibrium. The rate of mineralization of RhB was determined by taking small aliquots of the sample at different time intervals of sunlight exposure and recording UV-Vis absorption spectra in a quartz cuvette of unit path length. Rate constants for the degradation of RhB were calculated by using a first-order reaction rate equation:

$$\ln \frac{C_0}{C_t} = kt \tag{1}$$

where, k = pseudo-first-order rate constant (min^{-1}), C_0 and C_t are the concentrations at time = 0 min and t min, respectively. The value of k can be determined from the slope obtained by linear fitting of the plot between $\ln(C_0/C_t)$ and t.

The experiment was repeated four times to check the recyclability and photostability of the particles. To probe the mechanism of catalysis acquired by the catalyst, scavenging experiments were conducted to find the role of different reactive oxygen species (ROS) in the photodegradation of RhB dye. Aqueous solutions of benzoquinone (BQ) (0.5 mM), isopropyl alcohol (IPA) (5 mM), and disodium salt of ethylenediaminetetraacetic acid (EDTA) (5 mM) were added to the 0.01 mM aqueous solution of RhB along with the catalyst for scavenging $O_2^{\cdot -}$, $OH^{\cdot}$ and holes respectively. Then, the procedure of photocatalysis was repeated as done in the absence of a scavenger, and UV-Vis absorption spectra were recorded for each scavenging experiment to evaluate the comparative impact of ROS on RhB mineralization.

1.5 Calculation of Band potentials from Electronegativities: The band gaps (E_g) for JNP-1 and JNP-2 were determined from the Tauc plots (Figure S8).[1] From the values of E_g obtained for JNP-1 (4.05 eV) and JNP-2 (3.99 eV), band edge potentials are calculated by the methods previously reported[2] using the following equations:

$$E_{VB} = \chi - 4.5 + \frac{1}{2}E_g \tag{2}$$

$$E_{CB} = E_{VB} - E_g \tag{3}$$

Where, E_{CB} and E_{VB} are energy potentials for the conduction band and valence band respectively, and χ is the absolute electronegativity of AgBr determined from the geometric mean of absolute electronegativities of respective elements.[3] The values of E_{CB} and E_{VB} obtained from the above method are in reference to the Normal Hydrogen Electrode (NHE). The value of 4.5 is subtracted in equation (2) because on the Absolute Electrochemical Scale (AES) the level with 4.5 eV potential has a value of 0.0 eV in reference to the NHE.[4]

1.6 Antibacterial Activity Assay: Antibacterial activity of prepared AuAg alloy@AgBr JNPs was assessed using two Gram-negative (*Escherichia coli*, *Pseudomonas syringae*) and two Gram-positive (*Bacillus subtilis*, *Staphylococcus aureus)* bacterial strains. The assays were carried out as per Ennaas *et al.,*[5] with few modifications. 1 mg ml^{-1} samples were diluted to 2 folds in Luria Bertani (LB) broth. The samples were then seeded with 100 µL of bacterial suspension (approximately 1×10^6 CFU ml^{-1}) and were incubated overnight. The *E. coli* and *S. aureus* inoculated samples were kept at 37 °C, whereas *P. syringae* and *B. subtilis* were incubated at 28 °C and 30 °C, respectively. The antibiotic kanamycin was used as a reference. After 24 h, the optical density was taken at 600 nm. The inhibition percentage was calculated using the formula mentioned below:

$$Growth\ Inhibition\ \% = \frac{(Absorbance\ of\ control - Absorbance\ of\ sample)}{Absorbance\ of\ control} * 100 \quad (4)$$

The linear regression method was used to determine the minimum inhibitory concentration (MIC) values. MIC value corresponded to the X-intercept value of the curve plotted between the different concentrations of the given sample (X-axis) and their respective optical density at 600 nm (Y-axis). All the experiments were performed using three biological replicates and results were analyzed using one-way and two-way analysis of variance (ANOVA) (the Fischer LSD) (Sigma Stat version 3.5).

2. Annexure S2

2.1 Redox potentials of ROS: The redox potentials of the different ROS with respect to NHE are given below,[6]

$$O_2 + e^- \rightarrow O_2^{-\cdot},\ E^\circ = -0.18\ V \quad (5)$$

$$O_2 + e^- \rightarrow H_2O_2,\ E^\circ = 1.56\ V \quad (6)$$

$$H_2O_2 + e^- \rightarrow OH^\cdot,\ E^\circ = 0.8\ V \quad (7)$$

$$OH^\cdot + e^- \rightarrow H_2O,\ E^\circ = 2.73\ V \quad (8)$$

$$OH^\cdot + e^- \rightarrow OH^-,\ E^\circ = 1.9\ V \quad (9)$$

$$Br^\cdot + e^- \rightarrow Br^-,\ E^\circ = 1.96\ V \quad (10)$$

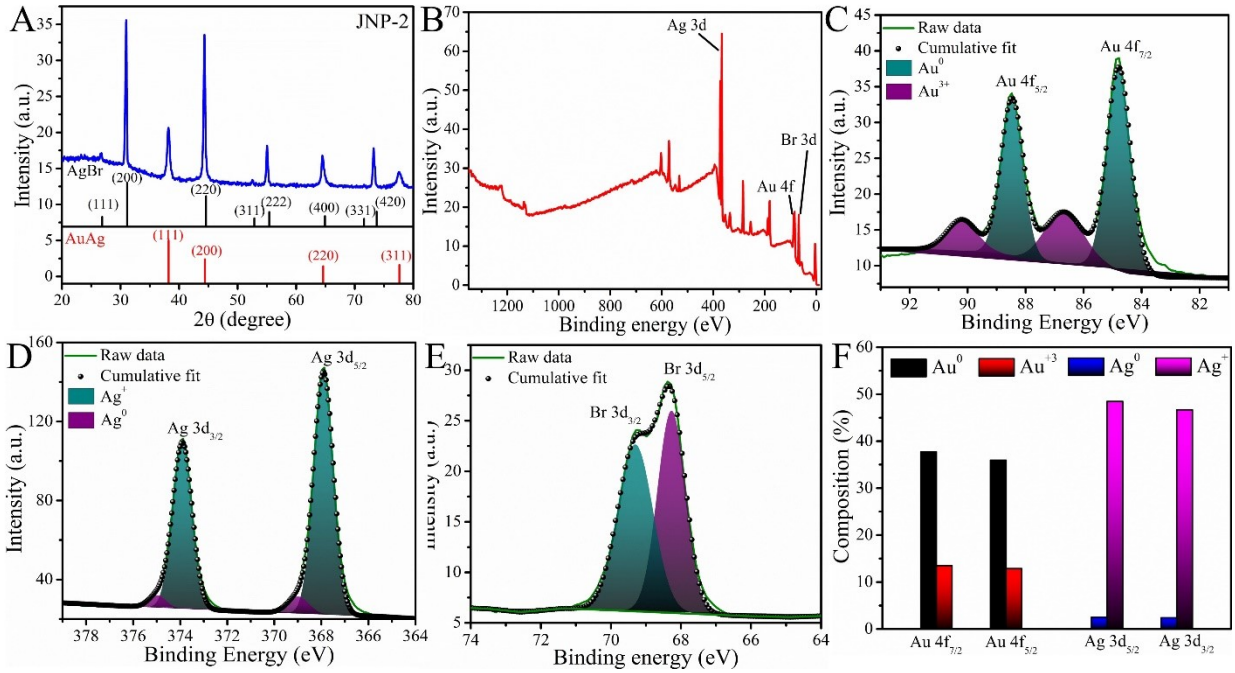

Figure S1: (A) XRD pattern; (B) XPS survey scan; (C-E) XPS spectra of Au, Ag, and Br elements; and (F) relative percentage composition of metallic and ionic Au and Ag in AuAg alloy@AgBr JNP-2.

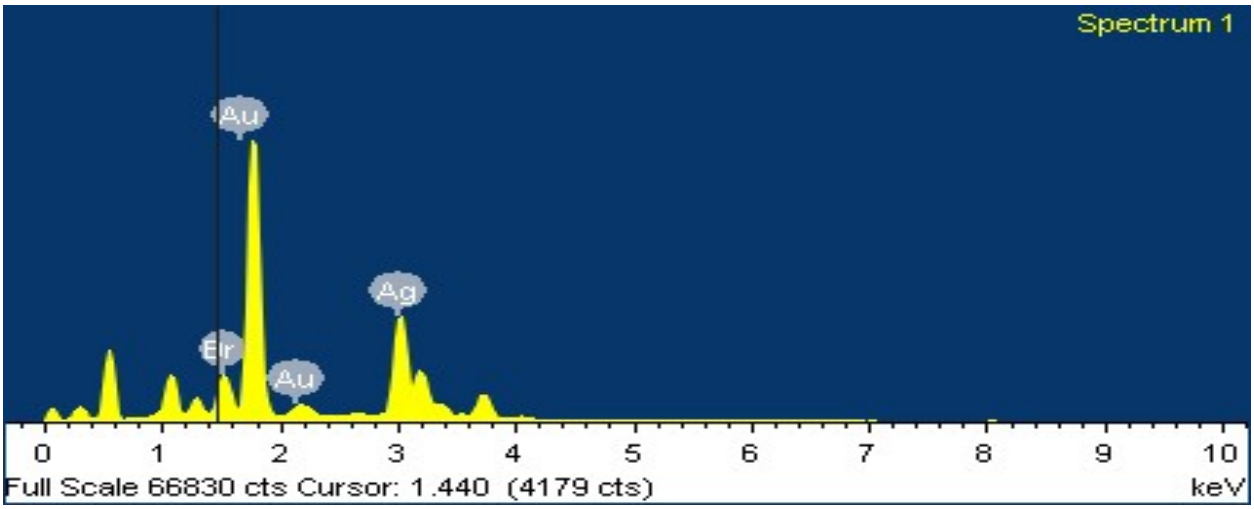

Figure S2: Energy dispersive X-ray (EDX) spectrum showing the presence of Au, Ag and Br in JNP-1 (The relative composition of the elements shown here is qualitative as a coating of Ag is done on over the cast sample prior to the measurement).

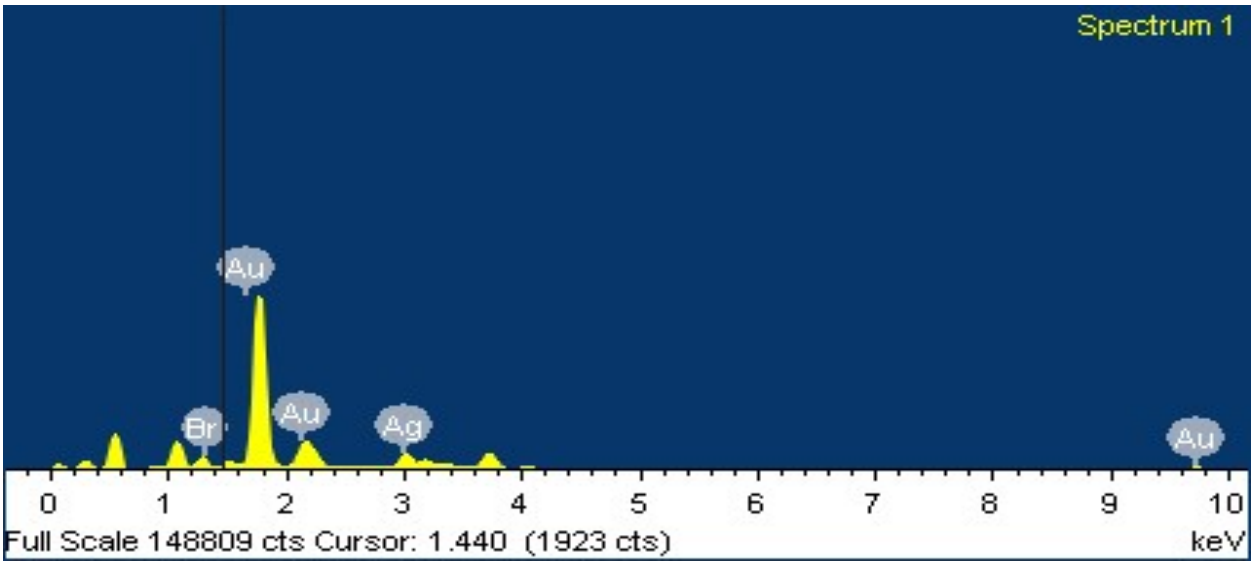

Figure S3: Energy dispersive X-ray (EDX) spectrum showing the presence of Au, Ag, and Br in JNP-2 (The relative composition of the elements shown here is qualitative as a coating of Ag is done on over the cast sample prior to the measurement).

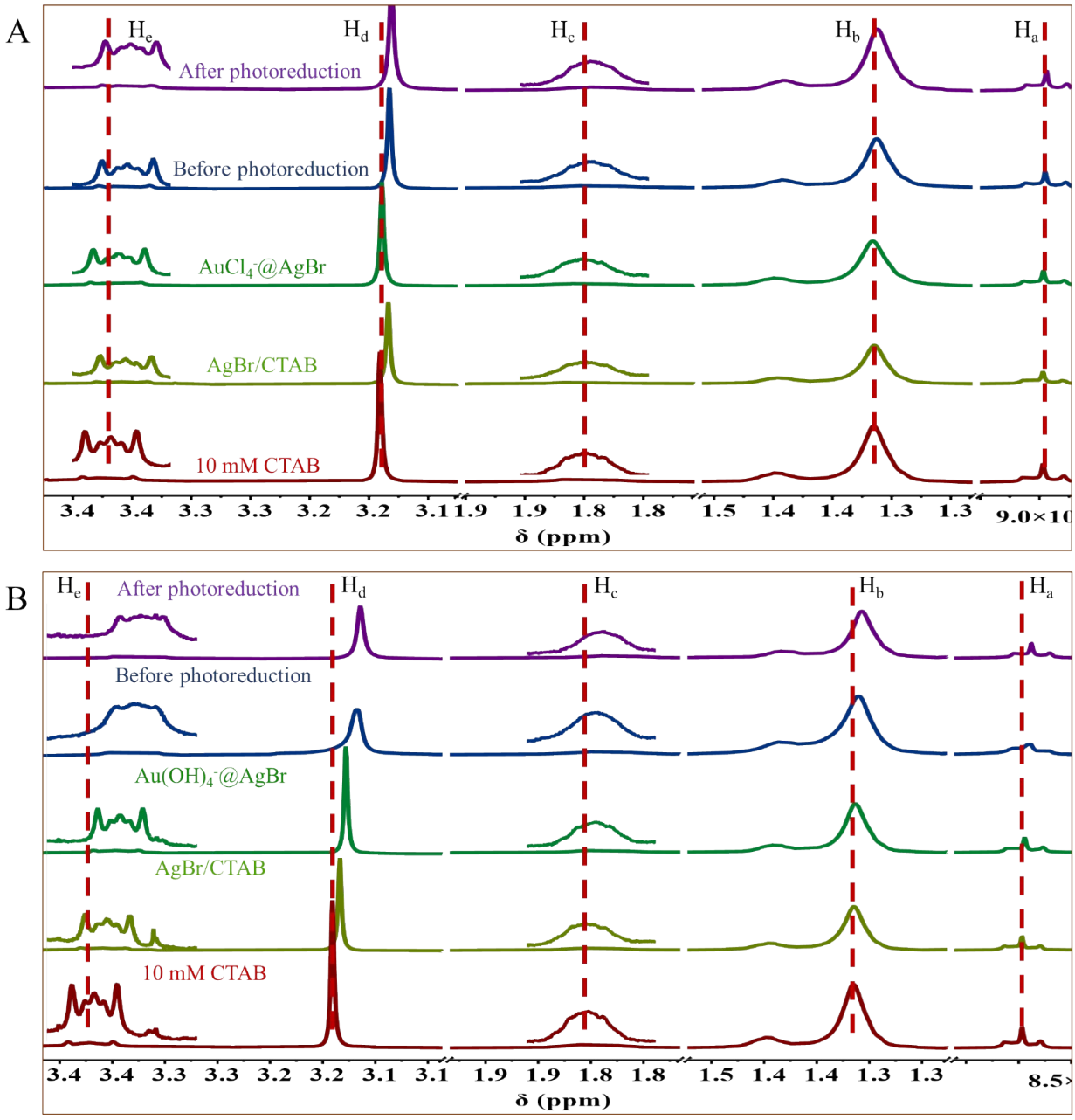

Figure S4: (A, B) NMR spectra of CTAB at different stages of preparation of JNP-1 and JNP-2 respectively.

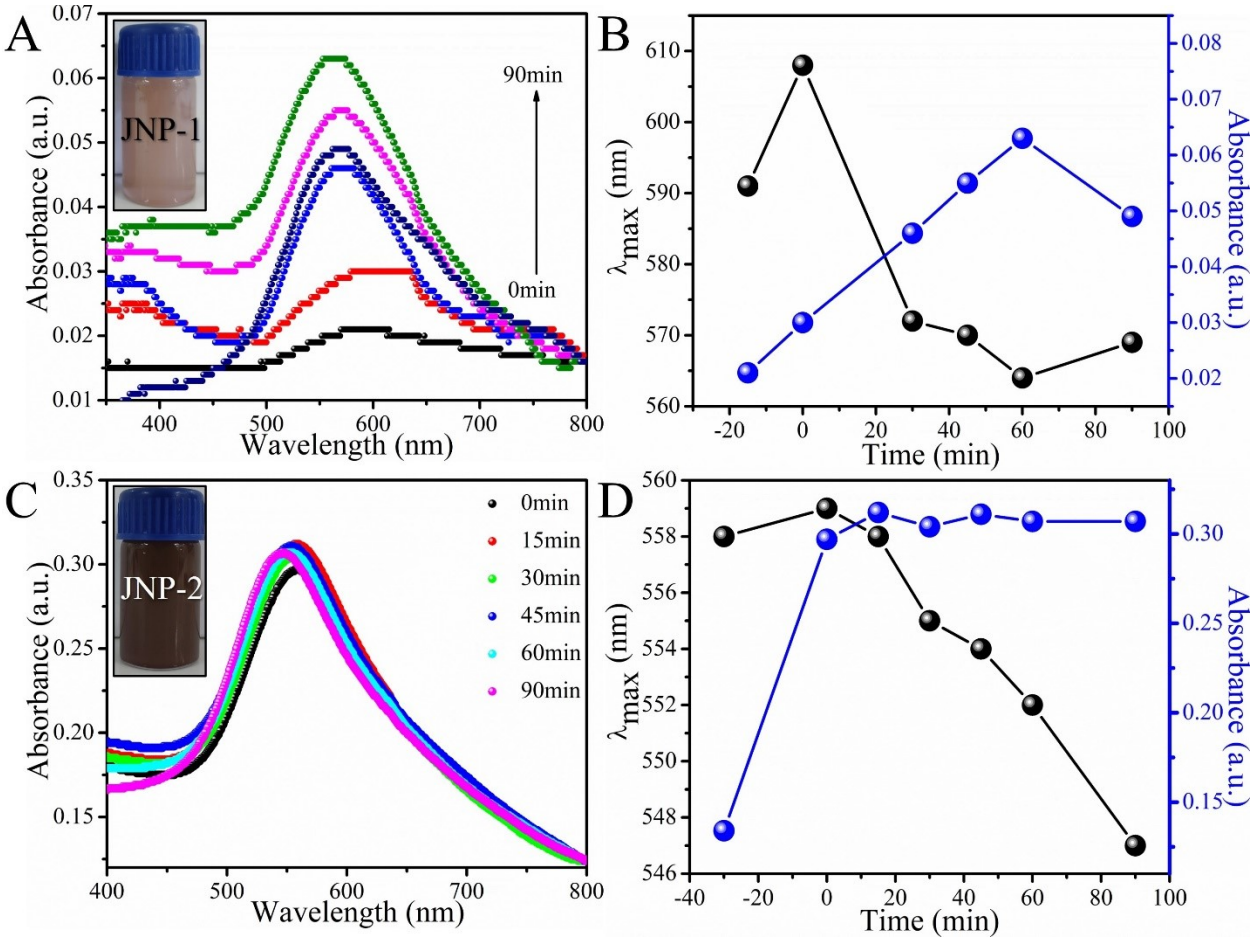

Figure S5: (A) Time-dependent UV-visible spectrum and (B) variation of absorbance and λ_{max} with time of sunlight exposure for JNP-1; (C) Time-dependent UV-visible spectrum and (D) variation of absorbance and λ_{max} with time of sunlight exposure for JNP-2. Insets of (A) and (C) show photographs of JNP-1 and JNP-2 prepared after photoreduction, respectively.

The growth of JNP-1 and JNP-2 is monitored by time-dependent UV-visible spectroscopy while irradiating under sunlight after the addition of ascorbic acid (Figure S4A-D). The observations revealed the predominant growth of the Au^0 phase over the Ag^0 phase while establishing that the JNP-1 (under acidic conditions) forms via photoreduction whereas JNP-2 (under basic conditions) takes the route of chemical reduction. The nucleation and growth mechanism of AuAg alloy@AgBr JNPs is supposed to be micelle-mediated and initially proceeds via step-wise reduction of Au^{3+}/ Au^{+} by ascorbic acid as the reducing agent aided by sunlight.

For both JNP-1 and JNP-2, no visible band corresponding to surface plasmon resonance of Ag^0 phase (~ 400-450 nm) further confirms the inferences gained from XPS spectroscopy about the predominant formation of Au^0 phase over Ag^0 phase. In the case of JNP-1, the SPR band of Au^0 is centered around ~ 590 nm, the absorption of which increases and then saturates after 60 minutes

of sunlight illumination. This suggests the growth of Au^0 onto the AgBr phase. The hyperchromic shift is accompanied by a blue shift in the SPR band, which shifts from 590 nm to 569 nm (Figure S4B) and pinpoints a decrease in the size of the growing particles.[7] On the other hand, in the case of JNP-2, a sharp SPR band centered ~ 558 nm appears after 15 minutes of the addition of ascorbic acid even under dark conditions (Figure S4D) which suggests the spontaneous chemical reduction pathway acquired in the basic medium as compared to photoreduction in acidic conditions. The SPR band that appeared under basic conditions exhibits a relatively smaller hyperchromic as well as blue shift as compared to that shown by JNP-1 upon irradiation under sunlight.

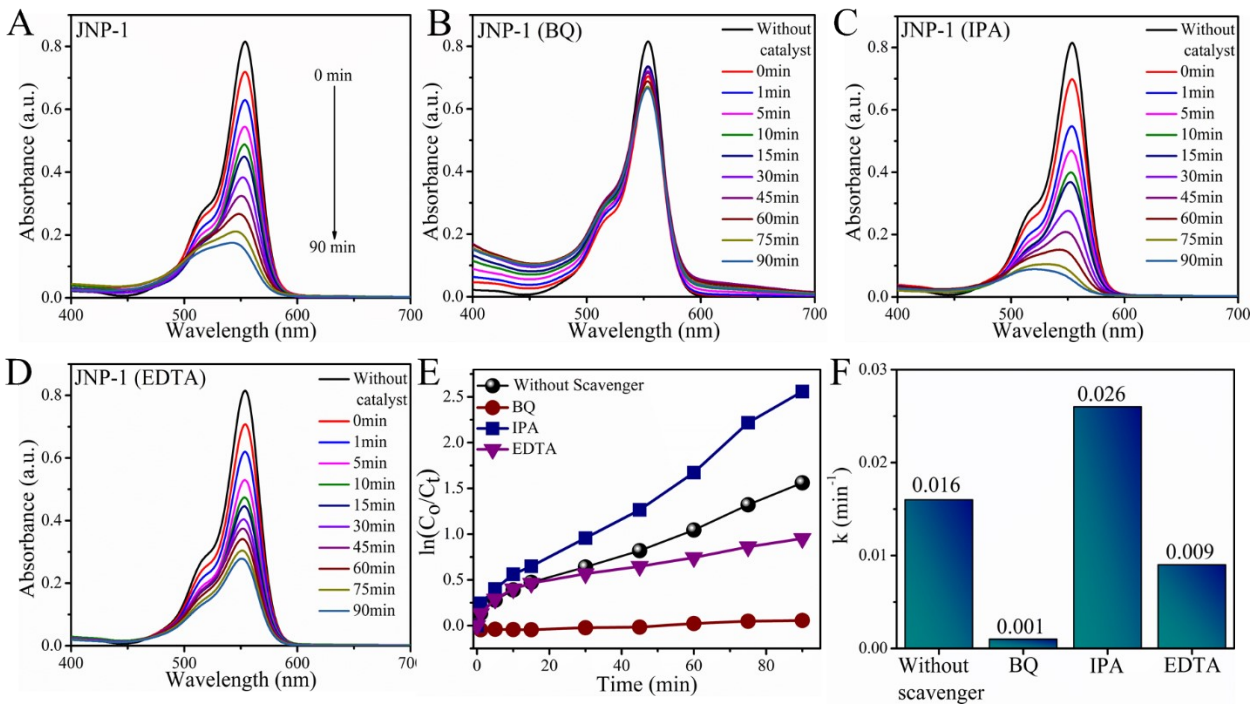

Figure S6: UV-Vis absorbance spectra of RhB in the (A) absence and (B-D) presence of BQ, IPA, and EDTA respectively; (E) Catalytic activity of JNP-1 under different circumstances; (F) Comparison of rate constant values of JNP-1 with different scavengers.

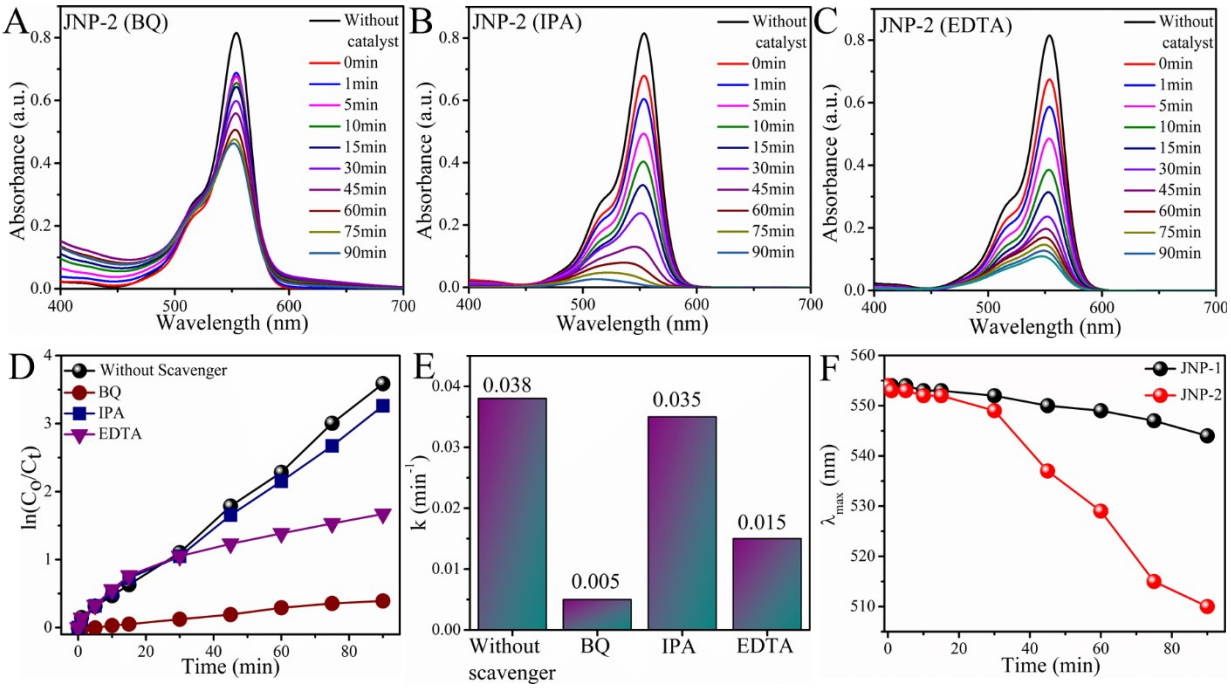

Figure S7: (A-C) UV-Vis absorbance spectra of RhB in the presence of BQ, IPA, and EDTA respectively; (D) Catalytic activity of JNP-2 under different circumstances; (E) Comparison of rate constant values of JNP-2 with different scavengers; and (F) Comparison of blue shift observed in case of JNP-1 and JNP-2.

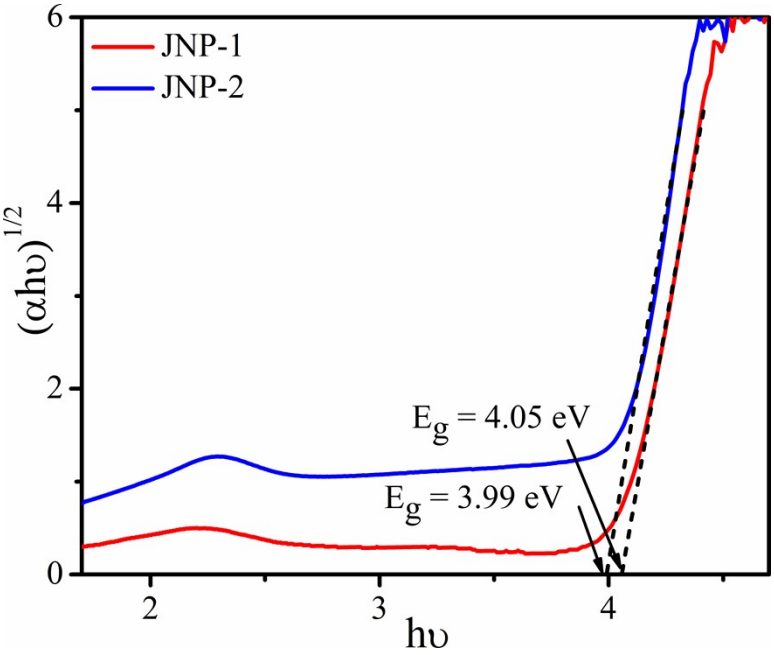

Figure S8: Tauc plots for the determination of band gap energy values for JNP-1 and JNP-2.

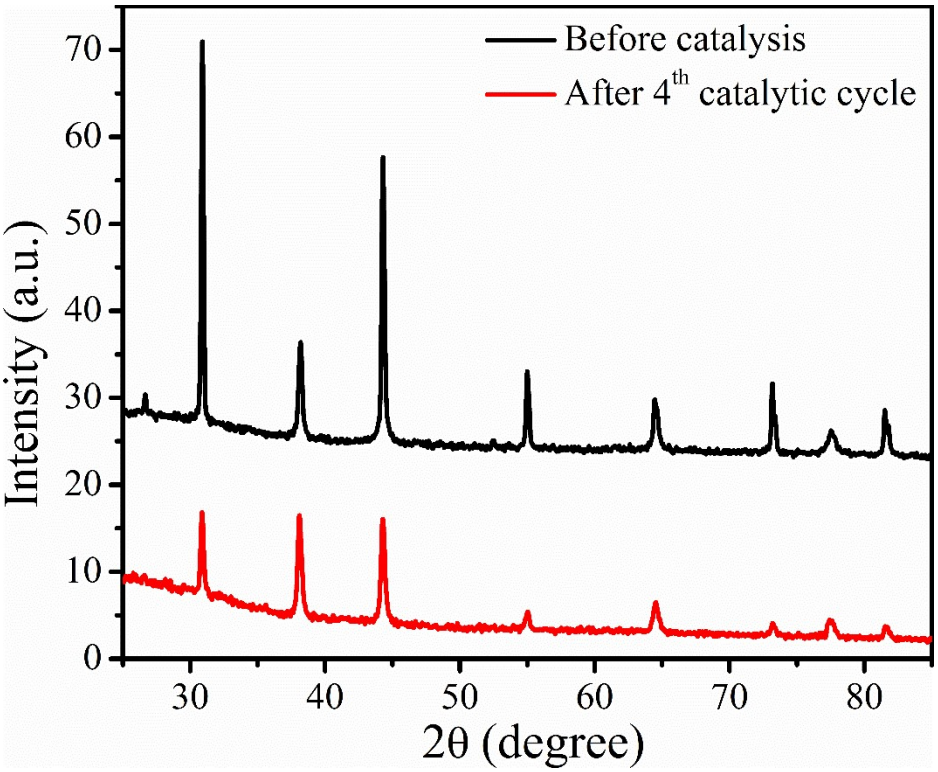

Figure S9: Comparison of XRD patterns of JNP-1 before and after photocatalysis.

Table S1: Antibacterial activity (% inhibition) of the JNPs with 0.5 mg/ml concentration against different bacterial strains.

Sample	*Escherichia coli*	*Pseudomonas syringae*	*Bacillus subtilis*	*Staphylococcus aureus*
DDW	1.78 ± 0.34^{d}	1.83 ± 0.30^{e}	1.58 ± 0.19^{f}	2.29 ± 0.79^{e}
Kanamycin	90.34 ± 0.71^{a}	89.53 ± 0.12^{a}	86.02 ± 1.59^{b}	82.14 ± 0.93^{b}
JNP-1	92.63 ± 1.68^{a}	88.45 ± 0.32^{a}	92.32 ± 1.03^{a}	90.00 ± 0.33^{a}
JNP-2	53.44 ± 1.01^{c}	49.26 ± 1.16^{c}	31.84 ± 0.26^{e}	29.47 ± 1.50^{d}

Data represents the Mean ± SE of three independent biological replicates. Different letters (a-f) within the column represent values that were significantly different among different samples (Fisher LSD, $p \leq 0.05$).

Table S2: Minimum inhibitory concentration (MIC) value of JNP-1 sample against different bacterial strains.

Bacterial strain	**Minimum inhibitory concentration (MIC) (µg ml^{-1})**
Escherichia coli	34.90
Pseudomonas syringae	35.53
Bacillus subtilis	42.64
Staphylococcus aureus	41.58

References:

1. P. Makuła, M. Pacia and W. Macyk, *J. Phys. Chem. Lett.,* 2018, **9**, 6814-6817.
2. M. A. Butler and D. S. Ginley, *J. Electrochem. Soc.,* 1978, **125**, 228.
3. A. H. Nethercot, *Phys. Rev. Lett.,* 1974, **33**, 1088-1091.
4. S. Sumi, T. Watanabe, A. Fujishima and K. Honda, *Bull. Chem. Soc. Jpn.,* 1980, **53**, 2742-2747.
5. N. Ennaas, R. Hammami, A. Gomaa, F. Bédard, É. Biron, M. Subirade, L. Beaulieu and I. Fliss, *Biochem. Biophys. Res. Commun.,* 2016, **473**, 642-647.
6. D. A. Armstrong, R. E. Huie, , W. H. Koppenol, , S. V. Lymar, G. Merényi, P. Neta, B. Ruscic, D. M. Stanbury, S. Steenken and P. Wardman, *Pure Appl. Chem.,* 2015, **87**, 1139-1150.
7. F. Kim, J. H. Song and P. Yang, *J. Am. Chem. Soc.,* 2002, **124**, 14316-14317.